Molecular Crystals and Liquid Crystals

Publication details, including instructions for authors and subscription information:
http://www.tandfonline.com/loi/gmcl20

A Nematic Liquid Crystal as an Amplifying Replica of a Holographic Polarization Grating

L. M. Blinov [a], G. Cipparrone [a], A. Mazzulla [a], C. Provenzano [a], S. P. Palto [b], M. I. Barnik [b], A. V. Arbuzov [b] & B. A. Umanskii [b]

[a] LICRYL - INFM Research Unit of Cosenza, Physics Department, University of Calabria, Rende (CS), Italy

[b] Institute of Crystallography, Russian Academy Science, Moscow, Russia

Version of record first published: 31 Aug 2006

To cite this article: L. M. Blinov, G. Cipparrone, A. Mazzulla, C. Provenzano, S. P. Palto, M. I. Barnik, A. V. Arbuzov & B. A. Umanskii (2006): A Nematic Liquid Crystal as an Amplifying Replica of a Holographic Polarization Grating, Molecular Crystals and Liquid Crystals, 449:1, 147-160

To link to this article: http://dx.doi.org/10.1080/15421400600583919

Mol. Cryst. Liq. Cryst., Vol. 449, pp. 147–160, 2006

ISSN: 1542-1406 print/1563-5287 online
DOI: 10.1080/15421400600583919

A Nematic Liquid Crystal as an Amplifying Replica of a Holographic Polarization Grating

L. M. Blinov
G. Cipparrone
A. Mazzulla
C. Provenzano
LICRYL – INFM Research Unit of Cosenza, Physics Department, University of Calabria, Rende (CS), Italy

S. P. Palto
M. I. Barnik
A. V. Arbuzov
B. A. Umanskii
Institute of Crystallography, Russian Academy Science, Moscow, Russia

Holographic gratings of different periods were recorded in the photopolymer by two laser beams with opposite circular polarization and a nematic liquid crystal was brought in contact with them. The anchoring conditions for the nematic were modulated in a similar way and an induced, field controlled replica manifested a characteristic asymmetric diffraction for the beams of opposite circular polarizations with dramatically enhanced diffraction efficiency. In fact the situation is more complicated than expected and our modelling of the director distribution for a finite anchoring strength explains the experimental data by considering an additional modulated structure at the polymer-nematic interface.

Keywords: electro-optics; holography; liquid crystals

This work was partially supported by Russian Fund for Basic research (project no. 03-02-17288). S.P. Palto is grateful to Russian Science Support Foundation. We also acknowledge the financial support from Cemif.cal.

Address correspondence to L. M. Blinov, LICRYL – INFM Research Unit of Cosenza, Physics Department, University of Calabria, Rende (CS), 87036, Italy. E-mail: blinov@fis.unical.it

1. INTRODUCTION

Polarization holographic gratings are very promising for image processors and spectral polarimeters [1,2]. A possibility for recording holographic gratings in organic films containing azobenzene chromophores has been shown in variety of papers, see e.g., [3–5]. Of particular interest are the gratings recorded by two laser beams with opposite circular polarizations. When such beams of equal intensity form small angles of $\pm\vartheta/2$ with respect to the film normal, in the corresponding interference pattern the intensity of light is almost constant, but the light electric vector **e** rotates upon translation along the x-direction parallel to the beam incidence plane (Fig. 1a).

In terms of the Jones vectors the distribution of field $E = E_R(x) + E_L(x)$ in the plane of the film along x can be written as follows (ϑ is assumed small):

$$E \cong E\left(\begin{vmatrix} \exp(-ikx\sin(\vartheta/2)) \\ \exp(i\pi/2 - ikx\sin(\vartheta/2)) \end{vmatrix} + \begin{vmatrix} \exp(ikx\sin(\vartheta/2)) \\ \exp(-i\pi/2 + ikx\sin(\vartheta/2)) \end{vmatrix}\right)$$
$$= 2E\begin{bmatrix} \cos(kx\sin(\vartheta/2)) \\ \sin(kx\sin(\vartheta/2)) \end{bmatrix} \quad (1)$$

where $k = 2\pi/\lambda$ is the wavevector modulus for incident waves of wavelength λ, E is the electric field amplitude of the two waves. The origin of our coordinate system ($x = 0$) is chosen to provide a zero phase shift

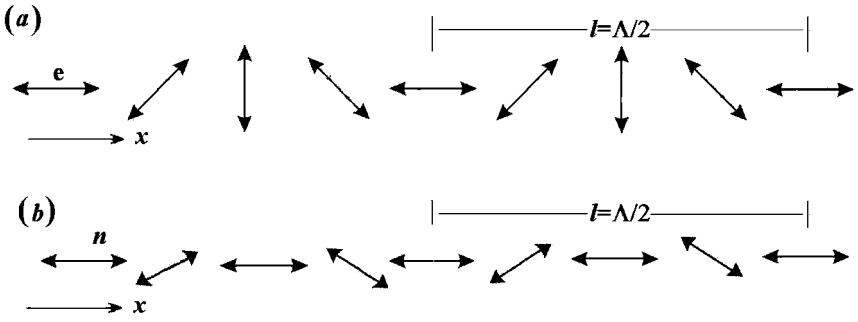

FIGURE 1 (a) Orientation of the light electric vector in the interference pattern formed by two circular, oppositely polarized beams. The induced optical axis in the photosensitive polymer and the director **n** of NLC (strong anchoring to the polymer) follow this orientation rotating upon the translation along x. (b) Orientation of the NLC director in another grating predicted by our modelling for weak director anchoring. In this case **n** oscillates about x without rotation, keeping it average position along x.

between the recording waves. According to Eq. (1) the electric field vector is oriented at an angle of $kx\ \sin(\vartheta/2)$ with respect to the x-axis, so it rotates with increasing x axis. The rotation of the field vector through 2π arises at a distance of Δx, which can be found from a condition $2\pi = k\Delta x\ \sin(\vartheta/2) = (2\pi\Delta x/\lambda)\sin(\vartheta/2)$. The value of $\Lambda \equiv \Delta x = \lambda/\sin(\vartheta/2)$ is just the full period for the 2π variation in the orientation of the recording electric field vector.

Such a field pattern can be recorded in a photosensitive material (e.g., azobenzene films [2,5]) by means of the photoinduced molecular orientation. Correspondingly the photo-induced optical axis in the medium follows the same law with the total period Λ. However, in our case the optical axis orientations differing for integer number of π are optically indistinguishable, and the grating pitch is twice shorter than the period Λ, namely $l = \Lambda/2 = \lambda_0/2\sin(\vartheta/2)$ (λ_0 is wavelength of recording beam). Such gratings manifest unique diffraction properties [6]. For example, for a normally incident linearly polarized wave with the electric vector parallel to the wavevector x of the grating, $\mathbf{E} = [E_x, 0]$, the diffracted field consists of three beams:

$$\mathbf{E}_d = J_f\mathbf{E} = E_x\begin{bmatrix}\cos\frac{\Delta}{2}\\ 0\end{bmatrix} + i\frac{1}{2}E_x\sin\frac{\Delta}{2}\begin{bmatrix}e^{-i\delta(x)}\\ e^{-i\delta(x)+i\pi/2}\end{bmatrix} + i\frac{1}{2}E_x\sin\frac{\Delta}{2}\begin{bmatrix}e^{i\delta(x)}\\ e^{i\delta(x)-i\pi/2}\end{bmatrix} \tag{2}$$

Here $\delta \equiv \delta(x) = 2kx\ \sin(\vartheta/2) = (4\pi x/\lambda)\sin(\vartheta/2)$ and Δ is phase retardation for the grating of thickness L and photo-induced optical anisotropy $n_a = n_e - n_o$, $\Delta = 2\pi L\ n_a/\lambda$. Therefore, we have the beam of zero order (transmission) and two diffracted beams of only $+1$ and -1 orders (without higher order diffraction). All the beam intensities are oscillating with increasing Δ.

When the same grating is illuminated by a circularly polarized beam, the diffraction become extremely asymmetric; only a single 1st order diffraction spot forms, either at an angle $+\vartheta'$ or $-\vartheta'$ depending on whether the reading beam is left- or right-polarized. The corresponding diffraction efficiency $\eta_\pm$ in these 1st order spots and the beam transmission T (0th order diffraction) are:

$$\eta_{\pm 1} \propto \sin^2(\Delta/2) = \sin^2(\pi L n_a/\lambda)$$
$$T \propto \cos^2(\Delta/2) = \cos^2(\pi L n_a/\lambda) \tag{3}$$

These equations predict anti-phase oscillations in $\eta_{\pm 1}$ on the one hand and T on the other when either layer thickness L or its birefringence n_a (or both) are varied. In the ideal case, the amplitude of the

oscillations reaches 1. The experiments made on thin films of an azobenzene dye with fixed L and Δn have confirmed [5] the main predictions of the theory. However, up to now there was not suggested any way to vary these important parameters for the same grating *in situ*.

The idea of the present work is based on the fact that holographic gratings recorded on some photosensitive materials provide a periodic alignment of nematic liquid crystals (NLC) [7]. Thus we record the holographic gratings on a polymer composition insoluble in an NLC and bring the grating in contact with the liquid crystal. We expected that the unique properties of the polymer gratings will be transferred to the NLC and it would be possible to control the asymmetric diffraction by an applied electric field.

2. EXPERIMENTAL

Our experiments have been made on a hybrid structure, Figure 2, which consists of two glasses covered with transparent indium-tin

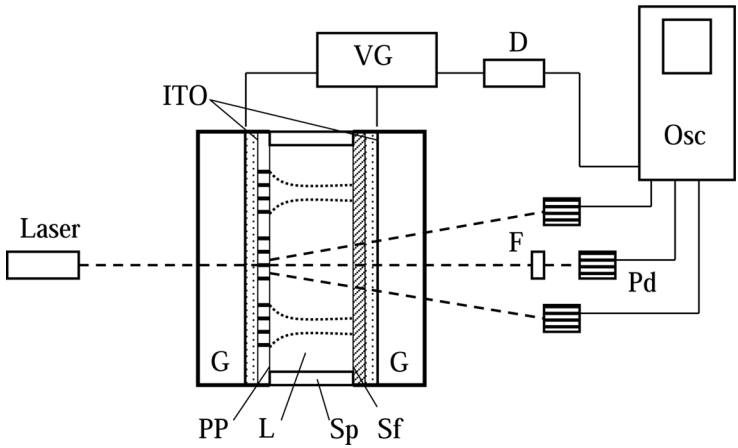

FIGURE 2 Geometry of a liquid crystal cell and the diffraction experiment. The liquid crystal cell consists of two glass substrates (G), covered by transparent electrodes (ITO) and either surfactant (Sf) or photosensitive polymer (PP) with recorded gratings. Spacers (Sp) form a gap filled with a liquid crystal (LC) (the orientation of the LC director at the grating position is schematically shown by dotted lines). Voltage applied to ITO electrodes from generator VG, after detector D is recorded by an oscilloscope (Osc). The intensities of the transmitted and diffracted beams of a He-Ne laser are measured by 3 photodiodes (PD) and the same oscilloscope. The laser is equipped with a pinhole and $\lambda/4$ plate for the beam geometry and polarization control, F is neutral filter.

oxide (ITO) electrode layer. A 20–30 nm thick photosensitive polymer layer (a mixture of polyimide and an azo-dye with the chemical formula and absorption spectra shown in Fig. 3) was spin-coated onto one electrode from a 2%-solution of the mixture in dimethylsulfamide and then baked for 1 h at 180°C. The gratings were recorded in this polymer composition by two circular, oppositely polarized beams of an Ar-ion laser at $\lambda = 457$ nm (power density 350 mW/cm^2, exposition time 120 s). The grating pitches were $l = 7.4$, 4.6 and 2.2 μm.

Due to small thickness and low absorption of the polymer layer at $\lambda = 457$ nm the diffraction efficiency of the polymer gratings was very low, $\eta \approx 10^{-6}$. They were even not seen under a polarizing microscope. In order to form an NLC cell the opposite, not patterned ITO electrode was covered by a surfactant (chromium distearylchloride) and the two glass substrates were separated by Mylar spacers. A cell gap d of either 13 μm or 26 μm was fixed and filled with a nematic mixture E7 (BDH) in the isotropic phase. The liquid crystal acquired a special orientation, homeotropic at the not patterned electrode and planar with modulated direction at the gratings. Between the gratings the

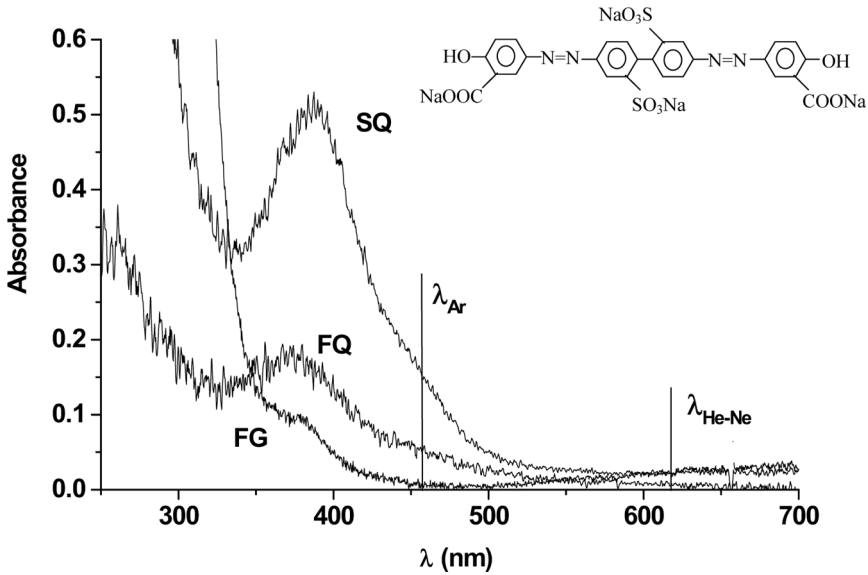

FIGURE 3 Chemical formula of P4G and absorption spectra of the 1:1 dye-polyimide mixture. Curve SQ: 2% dimethylformamide solution in a 6 μm thick quartz micro-cuvette. Curve FG: a thin film deposited onto the ITO-glass substrate used for grating recording. Curve FQ: a thicker film of the same composition deposited onto a quartz substrate.

NLC orientation was planar without any preferred axis. Under a microscope a multi-domain texture was observed.

For the measurements of diffraction efficiency a beam of a 4 mW He-Ne laser ($\lambda = 0.633\,\mu m$) either linearly or right/left circularly polarized was directed onto a particular grating. With the liquid crystal cell, we observed ± 1 or ± 2 and even ± 3 orders of diffraction depending on the grating pitch (2.2, 4.6, or 7.4 μm). The intensities of the zero-order (transmitted) and two 1st order diffracted beams for each particular grating were simultaneously recorded as functions of time by three identical photodiodes and a four-channel digital oscilloscope (Tektronix, model TDS 7104). All the three beams were either transmitted through pinholes or focused by lenses to study the role of light scattering. Different filters provided linear response of the photodiodes. No analyzer was used unless it is not specially said. During the time scan a sine-form voltage of frequency 5 kHz and variable amplitude $U_{rms} = 0$–7 V (sometimes up to 40 V) was applied to the cell electrodes. The a.c. response was converted into the d.c. signal by a simple detector and recorded by the same oscilloscope. Then recorded light intensities were plotted as functions of the a.c. voltage amplitude.

3. RESULTS

All our experiments were carried out on two cells, with an NLC layer 26 and 13 μm thick. The two cells manifest some specific features and we present these results one after another.

Thick Cell ($d = 26\,\mu m$)

Figure 4 shows the diffraction efficiency of the grating with a pitch of $l = 7.4\,\mu m$ for the 0th (T_{foc}) and ± 1st orders ($\eta_{\pm 1}$) for a reconstructing beam with a linear polarization perpendicular to the wavevector of the grating. First of all this curve shows that in the limit of high voltage ($U_{rms} > 50$ V from the signal generator with an additional amplifier) the diffraction efficiency vanishes. This is expected because, at this voltage, the field coherence length [8] $\xi = E^{-1}(4\pi K/\varepsilon_a)^{1/2}$ is already about 0.2 μm, the overwhelming part of the NLC layer is already homeotropic (except interface layer $L \approx 0.2\,\mu m$ with a negligible phase retardation $\Delta \approx Ln_a/\lambda \approx 0.014\pi$) and no diffraction is possible. For our estimations we use $E = U_{rms}/300d$ in the Gauss system, $d \approx 26\,\mu m$, $\varepsilon_a \approx 14.5$, elastic modulus $K \approx 10^{-6}$dyn, $n_a = 0.21$, $\lambda = 0.633\,\mu m$.

The diffraction efficiency is quite high, about 5–7% at maximum and this value exceeds the diffraction efficiency of the polymer grating by more than 4 orders of magnitude. A difference between η_{+1} and η_{-1}

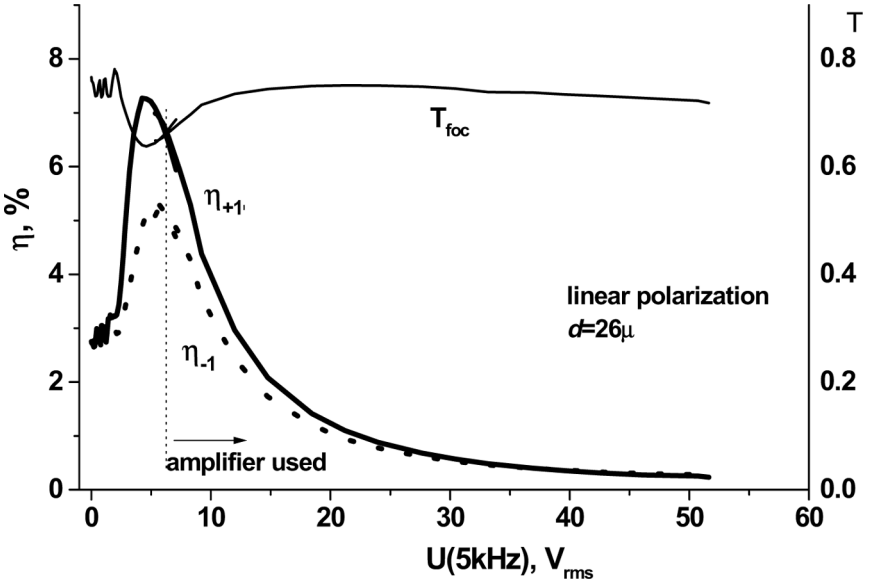

FIGURE 4 Dependencies of optical transmittance T and diffraction efficiency for $+1$ order (solid curves) and -1 order (dotted curves) on the applied voltage of frequency 5 kHz for the cell of thickness $d = 26\,\mu$m with a gratings of $l = 7.4\,\mu$m pitch (linear light polarization, the transmitted beam is focused onto the photodetector).

is not large and becomes even smaller when the sample is rotated about the laser beam. The transmittance manifests 4 full oscillations in anti-phase with respect to the diffracted beams. All of them are at voltages lower than 8 V, therefore further experiments were carried out in the range of 0–8 V_{rms}. The largest oscillation in T_{foc} at 5 V is quite deep, about 15% despite no analyzer was installed and the transmitted beam was focused onto the detector to reduce the role of the light scattering.

For circularly polarized beams the efficiencies of the $+1$st and -1st orders are interchanged for the right and left polarizations. This is exactly what is expected for the diffraction by grating shown in Figure 1a. The maximum of diffraction efficiency of 14% is observed for the right circular polarization at U = 5 V but the maximum ratio $R_R = \eta_{-1}/\eta_{+1} = 2.3$ (for the right polarization) was not large. In this experiment the beams were focused onto the correspondent photodiodes by lenses therefore, due to the light scattered by structure inhomogeneities (domains), the oscillations in diffracted intensity

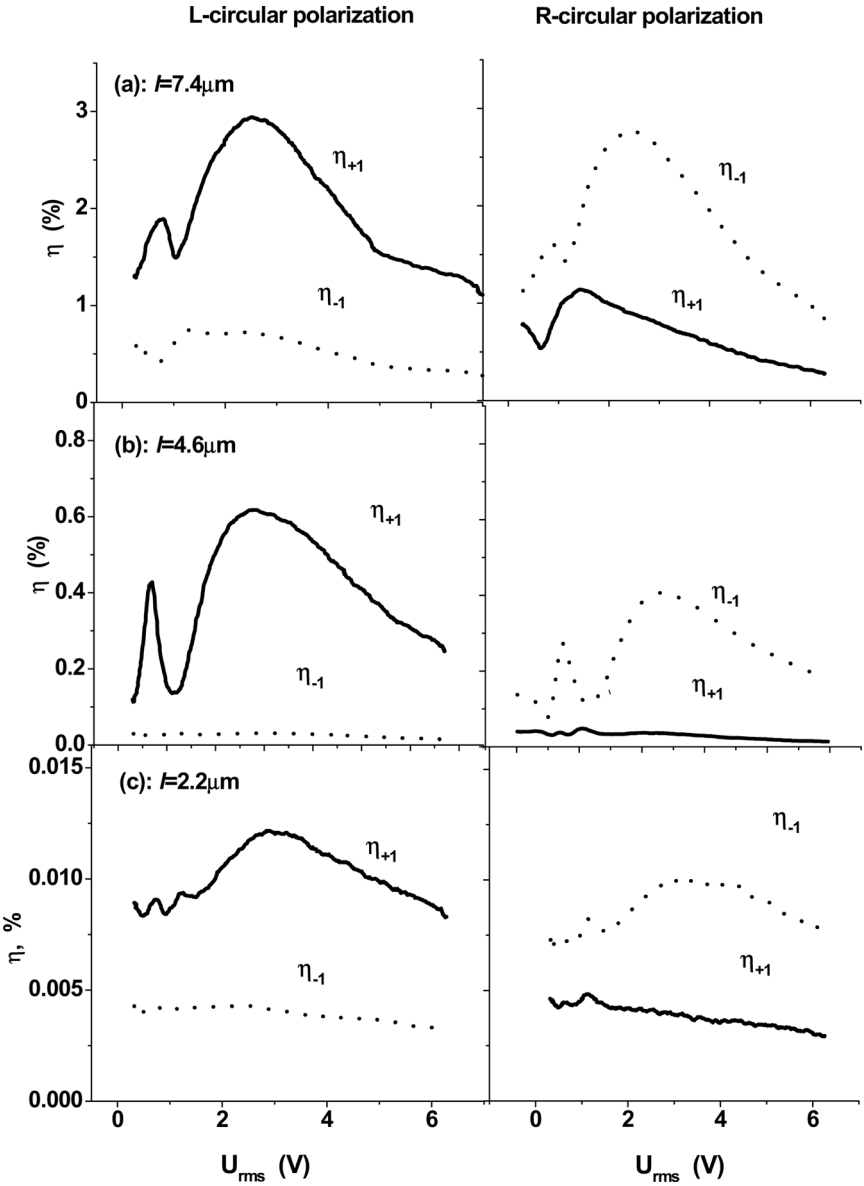

FIGURE 5 Dependencies of diffraction efficiency for +1 order (solid curves) and –1 order (dotted curves) on the applied voltage of frequency 5 kHz for three gratings with different pitch: $l = 7.4\,\mu$m (a), 4.6 μm (b) and 2.2 μm (c). Left and right columns correspond to left and right circular polarization of the reconstructing beam, cell thickness $d = 13\,\mu$m.

are not deep. Another situation is observed when we limit our beams with pinholes. Now the light scattering is considerably reduced and the beam intensities show deeper oscillations with $R_R = \eta_{-1}/\eta_{+1} \approx 9$ and $R_L = \eta_{+1}/\eta_{-1} \approx 4$. Strong asymmetry of diffraction and its oscillatory character point to that type of the diffracting structure (Fig. 1a) we are looking for. However the number of the observed oscillations seems to be too large for a replica formed close to the polymer surface. To consider this problem quantitatively we should first look at a thinner cell and gratings of different pitch.

Thin Cell ($d = 13\,\mu m$)

Figure 5a shows field dependence of diffraction efficiency ($\eta_{\pm 1}$) for $+1$ and -1 order spots for the grating having pitch $l = 7.4\,\mu m$. For the thinner cell the curves have again the oscillating character but with smaller number of oscillations. In this case the incident beam passed through a pinhole and the field induced maximum diffraction efficiency is 3%. In a stronger field ($U_{rms} \approx 40\,V$) the diffraction is not observed. As in the case of $26\,\mu m$ thick cell, for the left circular polarization (left-side plot) the diffraction efficiency for the $+1$ order markedly exceeds the efficiency for the -1 order (more than 3 times at the maximum). For the right circular polarization the situation is inverted (right-side plot). For a linear polarization parallel or perpendicular to the grating wavevector there is no such asymmetry.

For the grating with a shorter pitch of $l = 4.6\,\mu m$ the picture is the same, see Figure 5b, but the diffraction efficiency decreases down to $\eta_{max} \approx 6{\cdot}10^{-3}$ also the ratio $R_L = \eta_{+1}/\eta_{-1}$ is very high (at $U = 5\,V$ $R_L = 20$). For the grating with a pitch of $l = 2.2\,\mu m$, Figure 5*c* the diffraction efficiency decreases even more dramatically, $\eta_{max} \approx 1{\cdot}2.10^{-4}$, and the exchange by intensities between the ± 1 diffraction orders for different L- and R-polarizations is not so pronounced In n the thicker cell ($d = 26\,\mu m$) for $l = 2.2\,\mu m$ such an exchange has not been observed at all. As to the transmitted beam, with increasing field its intensity shows 1.5 full oscillations independently of the reconstructing beam polarization and grating pitch.

4. DISCUSSION AND MODELLING

Our observations result in an important conclusion: in many aspects the liquid crystal behaves as a replica of the grating recorded on the photosensitive polymer. Indeed, the local optical axis of the photopolymer layer behaves as an easy axis for the NLC alignment. If the anchoring energy of the NLC director at the polymer surface is strong,

near the polymer-NLC interface, within a layer of thickness L, the liquid crystal director orientation would follow the picture shown in Figure 1a i.e., acquire locally planar orientation with rotation in the substrate plane. Then, due to high positive dielectric anisotropy of E7 ($\varepsilon_a \approx 14.5$) an increasing field increases the homeotropically oriented part of the NLC at the cost of the thickness of the modulated layer and this is the reason for the field effect on the diffraction efficiency.

In Figure 6 we present the results of our modelling of the director distribution i.e., of the angle ϑ between the director and the normal to the NLC layer along the thickness of a 13 μm hybrid cell for

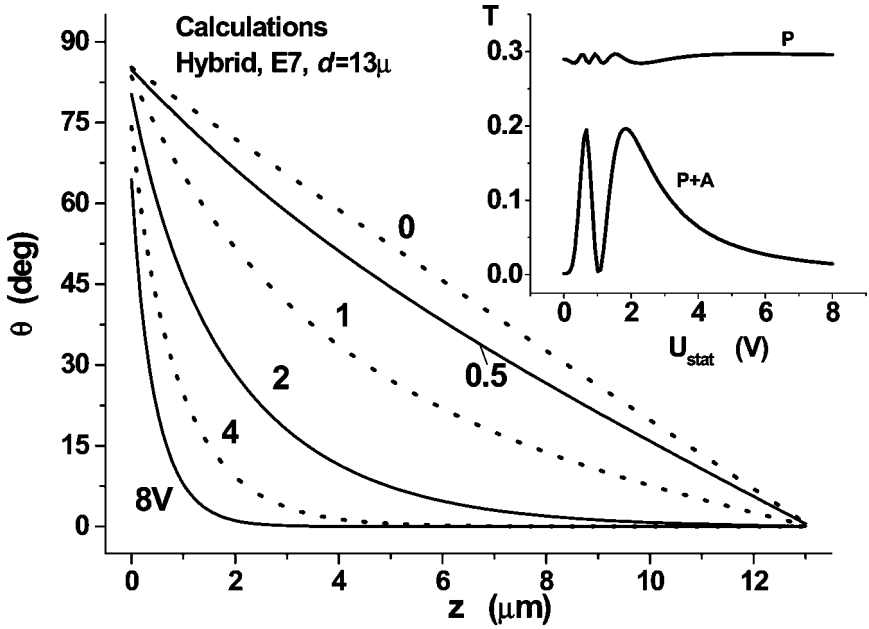

FIGURE 6 Results of modelling the director distribution (angle ϑ between the director and the normal to the NLC layer) along the thickness of a 13 μm hybrid cell for different voltages in the range of 0–8 V shown at the curves. Insert: voltage dependence of the cell transmittance between crossed standard polarizers (curve P + A), and in the absence of analyzer (curve P). The angle between P and the x-axis is $\pi/4$. Parameters of the cell and E7 mixture used in calculations: ($d = 13$ μm, dielectric constants $\varepsilon_\perp = 5.1$, $\varepsilon_{||} = 19.6$, refraction indices $n_\perp = 1.517$, $n_{||} = 1.735$ at $\lambda = 633$ nm, elastic moduli $K_{1,2,3} = 12$, 9 and 10 pN, anchoring energy 0.1 mJ/m^2 at both planar and homeotropic interfaces).

different voltages applied. In this case, uniform planar anchoring along x at $z = 0$ and homeotropic at $z = 13\,\mu m$ is assumed (no grating) and "one-dimensional" modelling based on the software developed earlier [9,10] was sufficient. The main plot in Figure 6 shows how the front of the homeotropic orientation moves under a field action and we see that, already at $U = 8\,V$, the director is parallel to the cell normal ($\vartheta = 0$) everywhere except a layer about $1\,\mu m$ thick near the planar interface. The transmittance-voltage dependence is shown in the Inset to Figure 6. When the cell is between crossed polarizers, we observe almost two full oscillations of transmittance with increasing voltage, curve P + A, corresponding to a phase retardation change by 3.83π (from $\Delta = 2\pi\langle n_a\rangle d/\lambda \approx 3.97\pi$ to 0.14π). When the analyzer is not used (curve P) the oscillations are very shallow and their number increases up to four because now they are originated from the light reflections from the cell boundaries. For the $26\,\mu m$ cell, due to lower field strength the calculated field-induced change in the phase retardation is about 7π.

These results would help us to understand the experimental plots if we consider the case when the NLC anchoring at the polymer grating is spatially modulated. Figure 7 shows the result of our calculation of the same ϑ-angle for the director in a particular place where the gratings shown in Figure 1a are recorded. In this case we used a new, "three-dimensional" modelling software developed recently by S.P. Palto, which will be described in a separate paper. Both the azimuthal and zenithal components of the anchoring energy are supposed to be quite strong ($0.05\,mJ/m^2$). Evidently, that due to the in-xy-plane rotation of the director at $z = 0$ and strong elastic torques competing with the spatial modulation of the director, the modulated part cannot spread into the whole volume, but occupied a part of it depending on the grating pitch. This is exactly what we see in Figure 7. Curve 1 is the same zero field curve shown in Figure 6. It corresponds to the infinite grating pitch, Curves 2 and 3 show the θ-distribution for the director on gratings with pitch $l = 7.4$ and $4.6\,\mu m$, respectively. With the known formula $n_e(\vartheta) = n_{\|}n_{\perp}/(n_{\|}^2\cos^2\vartheta + n_{\perp}^2\sin^2\vartheta)^{1/2}$ for the extraordinary refraction index we can calculate the optical anisotropy $n_a(\vartheta) = n_e(\vartheta) - n_{\perp}$, then by integrating over z we find $\langle n_a\rangle$ over cell thickness and the corresponding phase retardation. The result is: $\Delta = 2.0\pi$ and 1.2π for gratings with pitch $l = 7.4$ and $4.6\,\mu m$, respectively.

Therefore, with increasing field up to $U = 8\,V$ we expect one full oscillation in the transmittance for $l = 7.4\,\mu m$ or a half of the whole oscillation for $l = 4.6\,\mu m$. This is in contrast with our experiment, because in Figures 4 and 5 we observe four and two full oscillations

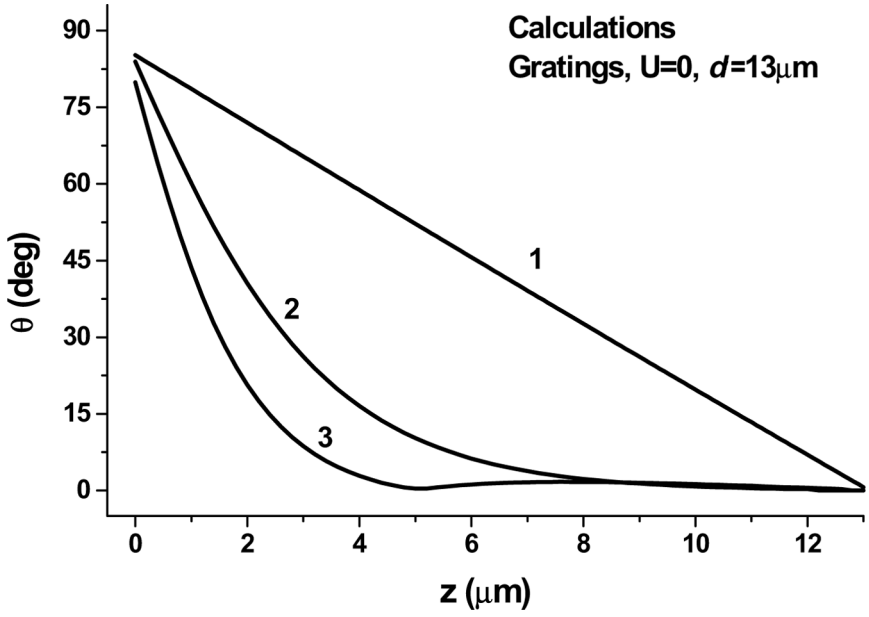

FIGURE 7 Results of modelling the zero-field director distribution along the thickness of the 13 μm cell with the gratings of type shown Figure 1a recorded on the polymer (opposite substrate provides homeotropic orientation). Curve 1 is the same zero field curve presented in Figure 6. Curves 2 and 3 show the θ-distribution for the director strongly anchored at gratings with pitch $l = 7.4$ and 4.6 μm, respectively.

independently of the grating pitch. In fact, our experiment corresponds to curve 1 in Figure 7. Another problem is related to diffraction efficiency, which, despite it is quite large, is still much less than expected. The additional problem arises with the 2nd and 3rd diffraction orders observed in experiment although in the ideal case of the grating shown in Figure 1a they should absent.

To understand this discrepancy with the naive model based on the periodic infinite anchoring strength we have simulated this situation. In the numerical simulation we can vary the in-plane azimuthal (within the substrate plane) anchoring energy W_a or corresponding surface extrapolation length [8], $b_a = K/W_a$. Our modelling shows that, *for weak anchoring* of $W_a \approx 0.01$–$0.001\,\mathrm{mJ/m^2}$, when $b_a > l$, it is more profitable for the director to deviate from the easy axis or even to break the anchoring in order to gain elastic energy. The formation of the replica with a structure shown in Figure 1a becomes unprofitable

and another type of the director distribution forms (formally, it means the existence of another solution of the Frank-Ericksen equations). In the new structure the NLC director instead of the full rotation shows only small local deviations $\sim\delta\phi$ from the x-axis. Very schematically such a structure is shown in Figure 1b. It is seen that the director distribution becomes biased along the grating wavevector and this explains the observed number of oscillations on the voltage-transmittance curves. This was also controlled experimentally: by rotation of the sample about the laser beam located at the center of a grating we clearly observe birefringence with the optical axis along the grating wavevector. The thickness of the modulated layer L for the new structure is very small $L \sim \delta\phi l/\pi$ that results in low efficiency $\eta_{\pm}$. This also explains why the efficiency of short pitch gratings reduces dramatically and why we observe 2nd and 3rd diffraction orders (they are not forbidden for the new grating). In fact the grating of the type shown in Figure 1a exists only as a part of the total grating area (about 1–10% for different pitches). We believe that the major part of our gratings has the structure shown in Figure 1b.

5. CONCLUSION

In conclusion, we have shown that the holographic gratings with unique diffraction properties, which are recorded in a photosensitive polymer by two circularly polarized beams with opposite polarization, can be "copied" , at least partially, by a liquid crystal brought in contact with the polymer. The liquid crystal grating shows the characteristic asymmetric diffraction of the circularly polarized reconstructing beam and is easily controlled by an external electric field. The diffraction efficiency of the spatially modulated structure induced in the liquid crystal can be four orders of magnitude higher than that of the photopolymer but still lower than expected. The latter can be explained by not sufficiently strong anchoring of the liquid crystal to the polymer grating resulting in a formation of a competing structure.

REFERENCES

[1] Todorov, T. & Nikolova, L. (1992). *Optics Letters*, *17*, 358.
[2] Cipparrone, G., Mazzulla, A., & Blinov, L. M. (2002). *J. Opt. Soc. Amer.*, *B 19*, 1157.
[3] Holme, N. C. R., Nikolova, L., Hvilsted, S., & Ramanujam, P. S. (1997). *Appl. Phys. Lett.*, *70*, 1518.
[4] Lagugnè Labarthet, F., Rochon, P., & Natanshon, A. (1999). *Appl. Phys. Lett.*, *75*, 1377.
[5] Cipparrone, G., Mazzulla, A., Palto, S. P., Yudin, S. G., & Blinov, L. M. (2002). *Appl. Phys. Lett.*, *77*, 2106.

[6] Nikolova, L. & Todorov, T. (1984). *Optica Acta*, *31*, 579.
[7] Blinov, L. M., Barberi, R., Cipparrone, G., Checco, A., Lazarev, V. V., & Palto, S. P. (1999). *Liq. Cryst.*, *26*, 427.
[8] Blinov, L. M. (1983). *Magneto-Optical and Electro-Optical Properties of Liquid Crystals*, J. Wiley: Chichester.
[9] Palto, S. P. (2001). *JETP*, *92*, 552.
[10] Palto, S. P. (2003). *Kristallografia*, *48*, 145.